Preprints of the 19th World Congress
The International Federation of Automatic Control
Cape Town, South Africa. August 24-29, 2014

Adaptive Inverse Output Feedback Control of Uncertain Systems Preceded with Hysteresis Actuators

Sining Liu and Chun-Yi Su

Department of Mechanical and Industrial Engineering, Concordia University, Montreal, Quebec H3G 1M8, Canada (e-mail: imsiningliu@gmail.com, cysu@alcor.concordia.ca).

Abstract: The development of control approaches for systems preceded with hysteresis nonlinearities has received great attentions in recent decades. The most common approach is the construction of an inverse model as the compensator to mitigate hysteresis effects. However, most of the developed schemes are state-based, requiring the availability of states of systems, which may not be the case for some practical systems. In this paper, output control with inverse compensation will be addressed. By using the inverse as a feedforward compensator for the model described by the modified generalized Prandtl-Ishlinskii (MGPI) model, an corresponding analytical expression of the inverse compensation error is first obtained. Then, an observer-based robust adaptive output feedback controller is developed. It is shown that the proposed output feedback control scheme can not only guarantee the stability of the control systems, but also can achieve the desired tracking accuracy.

1. INTRODUCTION

The hysteresis effects widely exist in smart material based actuators, such as piezoelectric actuators and magnetostrictive actuators. Such non-smooth nonlinearities usually confine the performance of the control systems with smart material based actuators Tao et al. [1995]. Control the systems preceded with the hysteresis effects becomes to an important topic and attractive challenge in the control system area. The most common approach is the construction of an inverse model as the compensator, which is pioneered by Tao and Kokotovic in Tao et al. [1995]. In order to construct the hysteresis inverse so as to facilitate the compensation, several mathematical hysteresis models have been proposed in the literature Mayergoyz [1991], Krasnoselskii et al. [1989]. The most accepted hysteresis models perhaps are the Preisach model, Prandtl-Ishlinskii (PI) model, and Bouc-Wen model. Among the above mentioned models, the PI model has a feature of its unique invertibility, which can be used as a feedforward compensator to mitigate the hysteresis effect in the control systems. In Al Janaideh et al. [2009], a generalized Prandtl-Ishilinskii model has been proposed to enlarge the application of the PI model, and a modified generalized Prandtl-Ishlinskii (MGPI) model has been introduced in Liu et al. [2013] to obtain the analytical inverse.

Using the inverses as feedforward compensators for the controller designs, the representative works can be found in, see, for example, Krejci et al. [2001], Tan et al. [2004], Chen et al. [2010]. In particular, in Liu et al. [2012] an adaptive variable structure controller has been developed along with the inverse construction for the MGPI model. The hysteresis nonlinearities and the tracking error of the dynamic system have been remedied successfully. However, most of the developed control methods in the literature are valid when the system states are measured. However, for a given particular dynamical system, in most of the case that the exactly knowledge of all the states is unavailable and the only accessible state is the output of the system. Therefore, it is significant to develop control schemes with observers to estimate the unavailable states from the measurements of a single outputZhou et al. [2012].

In this paper, an output control scheme still using inverse compensation will be addressed. First of all, the MGPI model is adopted for describing hysteresis nonlinearity and its corresponding inverse model is used as the feedforward compensator. Then, the analytical expression of the inverse compensation error is obtained to facilitate the controller design. Finally, an observer-based robust adaptive output feedback controller is developed for a class of uncertain systems preceded by a smart material based actuators. the proposed output control scheme guarantees the global stability of the close-loop control system as well as achieves the tracking accuracy. The effectiveness of the developed controller is illustrated by the simulation studies.

2. PROBLEM STATEMENT

2.1 System Model

Consider a controlled system consisting of a plant preceded by a hysteresis actuator (Su et al. [2005])

$$x^{(n)}(t) + \sum_{i=1}^{k} a_i Y_i(x(t),\dot{x}(t),\ldots,x^{(n-1)}(t)) = bu(t), y = x \tag{1}$$

$$u(t) = \Pi[v](t) \tag{2}$$

where Y_i are known continuous, linear or nonlinear functions. The parameters a_i and the control gain b are un-

known constants. It is a common assumption that the sign of b is known. Without losing generality, we assume that $b > 0$. Π is a hysteresis operator, which will be described in the later development. The function $u(t)$ is the output of hysteresis actuator (2), serving as the input signal of the nonlinear plant (1), and $v(t)$ is the input signal to the actuator.

When the states of the plant are unavailable except the system output $y(t)$, the control objective is to design a control law for $v(t)$ with unknown parameters of the system (1) and hysteresis (2), to drive the system output $y(t)$ to track a predefined desired trajectory, $y_d(t)$, i.e., $y(t) \to y_d(t)$ as $t \to \infty$.

Before proceeding, a basic assumption for $y_d(t)$ is required, which is standard and generally satisfied.

Assumption: The desired trajectory $\mathbf{y}_d = [y_d, \dot{y}_d, ..., y_d^{(n-1)}]^T$ is continuous. Furthermore, $[\mathbf{y}_d^T, y_d^{(n)}]^T \in \Omega_d \subset R^{n+1}$ with Ω_d being a compact set.

In this paper, focusing on the above control objective, an output control scheme with using inverse hysteresis cancelation will be developed. The proposed control scheme can be depicted in Fig.1

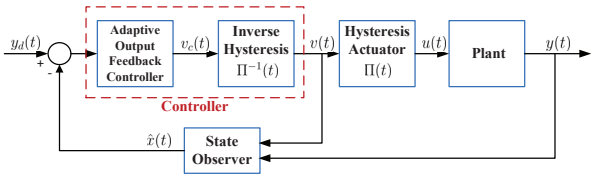

Fig. 1. Controller scheme

2.2 Modified Generalized Prandtl-Ishlinskii Hysteresis Model

To describe a general class of hysteresis shapes comparing to Prandtl-Ishilinskii (PI) model and to construct a corresponding analytical inverse, a modified generalized Prandtl-Ishlinskii (MGPI) model Liu et al. [2013] is adopted in this paper. The MGPI model is defined based on the weighted superposition of modified generalized play operators which are defined as follows. For any piecewise monotone input function $v(t) \in C_m[0, t_E]$ such that $v(t)$ is monotone on each of the subintervals $[t_i, t_{i+1}]$ where $i = 0, 1, \cdots, N-1$, the modified generalized play operator $w_M(t) = G_{mr}[v](t)$ with threshold $r \geq 0$ and initial value $w_{m_{-1}}$ is defined by

$$\begin{aligned} w_M(0) &= G_{mr}[v](0) = g_{mr}(v(0), w_{m_{-1}}), \\ w_M(t) &= G_{mr}[v](t) = g_{mr}(v(t), w_M(t_i)) \end{aligned} \tag{3}$$

where

$$g_{mr}(v, w_M) = max\{\gamma(v - r), min\{\gamma(v + r), w_M\}\} \tag{4}$$

for $t_i < t \leq t_{i+1}$, $0 \leq i < N$, where $\gamma(v)$ is an envelope function satisfying that $\gamma(0) = 0$ and strictly increasing.

Based on the definition (3), an MGPI model can be defined as

$$\Pi[v](t) = p_{m0}\gamma(v(t)) + \int_0^R p_m(r) G_{mr}[v](t) dr \tag{5}$$

where p_{m0} is a positive constant and $p_m(r)$ is an integrable density function. This density function satisfies $p_m(r) \geq 0$ with $\int_0^\infty r p_m(r) dr < \infty$. It represents the distribution of the weights for the modified generalized play operators with distinct thresholds r and vanishes when r is sufficient large. When we say the hysteresis is unknown, it implies the unknown p_{m0} and $p_m(r)$.

Following the similar procedure as shown in Liu et al. [2011], it can be verified that the proposed MGPI model $\Pi(t)$ fulfills the wiping out and the congruency properties as illustrated for the PI model.

3. THE INVERSE COMPENSATION

In Liu et al. [2013], the inverse of the MGPI model has also been constructed. In this section, the result of inverse MGPI model from Liu et al. [2013] will be briefly reviewed as follows.

3.1 The Inverse MGPI Model

Similar as in Liu et al. [2013], the MGPI model (5) with linear envelope function $\gamma(v) = m_0 v$, $m_0 > 0$ will be selected as an illustration.

The inverse MGPI model $\Pi^{-1}[v_c](t)$ can be constructed as

$$\Pi^{-1}[v_c](t) = \triangleq q_{m0} v_c(t) + \int_0^\infty q_m(s) F_s[v_c](t) ds \tag{6}$$

where s, q_{m0}, and $q_m(s)$ can be calculated as follows for the purpose of numerical implementation

$$s_i = p_{m0} m_0 r_i + \sum_{j=1}^{i} p_{mj} m_0 (r_i - r_j) \tag{7}$$

$$q_{m0} = 1/p_{m0} m_0 \tag{8}$$

$$q_m(s_i) = \frac{p_{mi} m_0}{(p_{m0} m_0 + \sum_{j=1}^{i} p_{mj} m_0)(p_{m0} m_0 + \sum_{j=1}^{i-1} p_{mj} m_0)} \tag{9}$$

for $i = 1, 2, \cdots, N$.

3.2 The Inverse Compensation Error

In this paper, an expression of the inverse compensation error will also be provided. As will be clear in late development, the benefit for such a design is that the inverse based controller with the inverse compensation error expression can achieve the tracking without necessarily adapting the uncertain parameters (the number could be large) in the hysteresis model, which achieves gain in computational efficiency.

Generally, the parameters of the MGPI model are not exactly available and their estimations are usually used. For the estimated MGPI model, the corresponding inverse $\hat{\Pi}^{-1}[v_c](t)$ is expressed by

$$\hat{\Pi}^{-1}[v_c](t) = \hat{q}_{m0} v_c(t) + \int_0^\infty \hat{q}_m(\hat{s}) F_{\hat{s}}[v_c](t) d\hat{s} \tag{10}$$

where $\hat{\Theta}^{-1}$ is the estimation of Θ^{-1} and $\hat{s}$, $\hat{q}_{m0}$ and $\hat{q}_m$ are calculated numerically through

$$\hat{s}_i = \hat{p}_{m0} m_0 r_i + \sum_{j=1}^{i} \hat{p}_{mj} m_0 (r_i - r_j) \tag{11}$$

$$\hat{q}_{m0} = 1/\hat{p}_{m0} m_0 \tag{12}$$

$$\hat{q}_{mi} = \frac{\hat{p}_{mi} m_0}{(\hat{p}_{m0} m_0 + \sum_{j=1}^{i} \hat{p}_{mj} m_0)(\hat{p}_{m0} m_0 + \sum_{j=1}^{i-1} \hat{p}_{mj} m_0)} \tag{13}$$

for $i = 1, \cdots, N$.

By using the result in Liu et al. [2012], the analytical form of the inverse compensation error can be first expressed as

$$e = (1 - \eta'(0)) v_c(t) - \int_0^\infty \eta''(r) F_r[v_c](t) dr. \tag{14}$$

where $\eta(r)$ is the composition of the initial loading curves of the MGPI model and it estimated inverse. Since the term $\int_0^\infty \eta''(r) F_r[v_c](t) dr$ in (14) is unbounded, which makes it difficult to directly apply the control approaches, an alternative expression of the inverse compensation error will be given to facilitate the controller design. Note that the play operator $F_r[v_c](t)$ in (14) can be rewritten in terms of the stop operator $E_r[v_c](t)$ (Brokate et al. [1006]).

Therefore, the inverse compensation error (14) can be further expressed as

$$\begin{aligned} e =& (1 - \eta'(0) - \int_0^\infty \eta''(r) dr) v_c(t) + \int_0^\infty \eta''(r) E_r[v_c](t) dr \\ \triangleq& (1 - \chi_0) v_c(t) + d[v_c](t). \end{aligned} \tag{15}$$

The boundness of $d[v_c](t)$ can be guaranteed by Wang et al. [2006], i.e., $|d[v_c](t)| \leq D$ where D is a bounded constant. Hence, $d[v_c](t)$ can be treated as a bounded disturbance. Based on this result, an adaptive output feedback controller $v(t)$ can then be designed to remedy the inverse compensation error as well as achieve the precise tracking.

4. STATE OBSERVER

Based on the result of (15) and available results Zhou et al. [2012] in the literature, design of an output feedback controller will be focused in the following development. As a first step, an state observer is required to construct.

To construct such an observer, the system (1) can be rewrite as

$$\dot{x} = Ax + \mathbf{a}^T \mathbf{Y} e_n + b u(t) e_n, \qquad y = cx \tag{16}$$

where

$$A = \begin{bmatrix} 0 & \\ \vdots & I_{n-1} \\ 0 & \cdots 0 \end{bmatrix}, \mathbf{a} = [\, -a_1 \cdots - a_k \,]^T, \mathbf{Y} = [\, Y_1 \cdots Y_k \,]^T,$$
$$c = [\, 1 \cdots 0 \,], e_n = [\, 0 \cdots 1 \,]^T \tag{17}$$

where Y_i are known continuous, linear or nonlinear functions. The parameters a_i and the control gain b are unknown constants. From (15), the output of the hysteresis actuator $u(t)$ with the inverse compensation (10) can be obtained by

$$u(t) = v_c(t) - e(t) = \chi_0 v_c(t) - d[v_c](t). \tag{18}$$

To construct an observer for (16), we choose $q = [q_1, \cdots, q_n]^T$ such that all eigenvalues of $A_0 = A - qc$ are at some desired stable locations. The estimate of $x(t)$ can be obtained by

$$\hat{x}(t) = \xi_0 - \sum_{i=1}^{k} a_i \xi_i + b\varrho \tag{19}$$

where

$$\begin{aligned} \dot{\varrho} &= A_0 \varrho + e_n u \\ \dot{\xi}_0 &= A_0 \xi_0 + q y \\ \dot{\xi}_i &= A_0 \xi_i + Y_i e_n, i = 1, \cdots, k \end{aligned} \tag{20}$$

It can be shown that the state estimation error $\epsilon = x(t) - \hat{x}(t)$ satisfies $\dot{\epsilon} = A_0 \epsilon$.

Note that the signal $u(t)$ is the output of the actuator, which usually can not be measured in the control systems in practice. Therefore, the signals ϱ in (20) is not available for controller design and need to be reparameterized. Let δ denote $(d)/(dt)$. With $\Lambda(\delta) \triangleq det(\delta I - A_0)$, we express $\varrho(t)$ as

$$\varrho = [\varrho_1, \cdots, \varrho_n]^T = [P_1(\delta), \cdots, P_n(\delta)]^T \frac{1}{\Lambda(\delta)} u(t) \tag{21}$$

for some known polynomials $P_i(\delta), i = 1, \cdots, n$. Note that $u(t) = \chi_0 v_c(t) - d(t)$ from (18), we obtain that

$$\varrho_i = \chi_0 \omega_i - d_i \tag{22}$$

where

$$\omega_i = \frac{P_i(\delta)}{\Lambda(\delta)} v_c(t), d_i = \frac{P_i(\delta)}{\Lambda(\delta)} d(t) \tag{23}$$

for $i = 1, 2, \cdots, n$. Based on (22), ω_i is available for controller design in place of $u(t)$.

In particular, denoting the second component of ξ_i as ξ_{i2}, $i = 0, 1, \cdots, k$, we have

$$\begin{aligned} \hat{x}_2 =& \xi_{02} - \sum_{i=1}^{k} a_i \xi_{i2} + b\chi_0 \omega_2 - b d_2 \\ \omega_2 =& \frac{\delta + q_1}{\delta^n + q_1 \delta^{n-1} + \cdots + q_n} v_c(t). \end{aligned} \tag{24}$$

5. ADAPTIVE OUTPUT FEEDBACK CONTROLLER DESIGN

With the inverse compensation error expressed in the form of (15) and the designed state observer (20), we are now ready to develop an adaptive output feedback controller to remedy the inverse compensation error as well as achieve the tracking accuracy. Note that in this section the adaptive control law will be designed for $v_c(t)$. The control signal $v(t)$ can then be calculated by $v(t) = \hat{\Pi}^{-1}[v_c](t)$ as described in (10).

First, some necessary definitions are given as follows

$$\begin{aligned} \tilde{\mathbf{a}} = \mathbf{a} - \hat{\mathbf{a}}, \quad \tilde{b} = b - \hat{b}, \quad \tilde{\phi} = \phi - \hat{\phi} \\ \tilde{D}_b = D_b - \hat{D}_b, \ \tilde{\chi}_b = \chi_b - \hat{\chi}_b, \ \tilde{\chi}_0 = \chi_0 - \hat{\chi}_0 \end{aligned} \tag{25}$$

where $\phi = 1/b$, $\chi_b = b\chi_0$ and $D_b = bD$. $\hat{\mathbf{a}}$, $\hat{b}$, $\hat{\phi}$, $\hat{\chi}_0$, $\hat{\chi}_b$, and $\hat{D}_b$ are the estimations of $\mathbf{a}$, b, ϕ, χ_0, χ_b, and D_b, respectively.

To design the output feedback controller through the backstepping approach, the following alternative coordinates are defined,

$$z_1 = y - y_d = x_1 - y_d \tag{26}$$
$$z_j = \hat{\chi}_0 \omega_2^{(j-2)} - \alpha_{j-1}, j = 2, 3, \cdots, n \tag{27}$$

where α_{j-1} is the virtual control at the jth step and will be determined in the later development.

Step 1: From (26) and (27), we can obtain that

$$\dot{z}_1 = \dot{x}_1 - \dot{y}_d = \xi_{02} + \mathbf{a}^T \xi_{i2} + b z_2 + b\alpha_1 + b\tilde{\chi}_0 \omega_2 - b d_2 + \epsilon_2 - \dot{y}_d \tag{28}$$

The first virtual control law α_1 is then selected as

$$\alpha_1 = \hat{\phi}\psi, \qquad \psi = -c_1 z_1 - l_1 z_1 - \xi_{02} - \hat{\mathbf{a}}^T \xi_{(2)} + \dot{y}_d \tag{29}$$

where c_1 and l_1 are positive constants and $\xi_{(2)} \triangleq [\xi_{12}, \xi_{22}, \cdots, \xi_{k2}]^T$.

The Lyapunov function candidate V_1 is chosen as

$$V_1 = \frac{1}{2} z_1^2 + \frac{1}{2\kappa_a} \tilde{\mathbf{a}}^T \tilde{\mathbf{a}} + \frac{|b|}{2\kappa_\phi} \tilde{\phi}^2 + \frac{|b|}{2\kappa_{\chi 0}} \tilde{\chi}_0^2 + \frac{1}{2l_1} \epsilon^T P_0 \epsilon \tag{30}$$

where κ_a, κ_ϕ and $\kappa_{\chi 0}$ are positive constants, and $P_0 = P_0^T > 0$ satisfies the equation $P_0 A_0 + a_0^T P_0 = -2I$. Substituting (29) into (28), the time derivative of V_1 is obtained by

$$\begin{aligned} \dot{V}_1 \leq & - c_1 z_1^2 + b z_1 z_2 + \frac{1}{\kappa_a} \tilde{\mathbf{a}}^T (\kappa_a z_1 \xi_{(2)} - \dot{\hat{\mathbf{a}}}) \\ & + \frac{|b|}{\kappa_{\chi 0}} \tilde{\chi}_0 (\kappa_{\chi 0} z_1 sgn(b) \omega_2 - \dot{\hat{\chi}}_0) \\ & - \frac{|b|}{\kappa_\phi} (\kappa_\phi z_1 sgn(b) \psi + \dot{\hat{\phi}}) - z_1 d_{b2} - \frac{3}{4l_1} \epsilon^T \epsilon \end{aligned} \tag{31}$$

where $d_{b2} \triangleq b d_2$ and $sgn(\cdot)$ represents the sign function. The adaptive laws for $\hat{\phi}$ and $\hat{\chi}$ are chosen as

$$\dot{\hat{\phi}} = -\kappa_\phi z_1 sgn(b) \psi \tag{32}$$

$$\dot{\hat{\chi}}_0 = \kappa_{\chi 0} z_1 sgn(b) \omega_2. \tag{33}$$

Step 2: From (27), we can obtain that

$$\begin{aligned} \dot{z}_2 = & z_3 + \alpha_2 + \dot{\hat{\chi}}_0 \omega_2 - \frac{\partial \alpha_1}{\partial y} (\xi_{02} + \mathbf{a}^T \xi_{(2)} + b\chi_0 \omega_2 - d_{b2} \\ & + \epsilon_2) - \frac{\partial \alpha_1}{\partial y_d} \dot{y}_d - \frac{\partial \alpha_1}{\partial \xi_0} \dot{\xi}_0 - \Sigma_{i=1}^k \frac{\partial \alpha_1}{\partial \xi_i} \dot{\xi}_i - \frac{\partial \alpha_1}{\partial \hat{\mathbf{a}}} \dot{\hat{\mathbf{a}}} \end{aligned} \tag{34}$$

Let KT_2 contain all the known terms in (34). The virtual controller α_2 is selected as

$$\begin{aligned} \alpha_2 = & - c_2 z_2 - l_2 (\frac{\partial \alpha_1}{\partial y})^2 z_2 - KT_2 + \frac{\partial \alpha_1}{\partial y} \hat{\mathbf{a}}^T \xi_{(2)} \\ & + \frac{\partial \alpha_1}{\partial y} \hat{\chi}_b \omega_2 - \hat{b} z_1 + \frac{\partial \alpha_1}{\partial \hat{\mathbf{a}}} \kappa_a (z_1 - \frac{\partial \alpha_1}{\partial y} z_2) \xi_{(2)} \end{aligned} \tag{35}$$

where c_2 and l_2 are positive constants.

The Lyapunov function candidate V_2 in this step is selected as

$$V_2 = V_1 + \frac{1}{2} z_2^2 + \frac{1}{2\kappa_b} \tilde{b}^2 + \frac{1}{2\kappa_{\chi b}} \tilde{\chi}_b^2 + \frac{1}{2l_2} \epsilon^T P_0 \epsilon \tag{36}$$

where κ_b and $\kappa_{\chi b}$ are positive constants. Substituting (35) into (34), we can obtain that

$$\begin{aligned} \dot{V}_2 \leq & - c_1 z_1^2 - c_2 z_2^2 + z_2 z_3 + \frac{1}{\kappa_a} \tilde{\mathbf{a}}^T (\kappa_a (z_1 - \frac{\partial \alpha_1}{\partial y} z_2) \xi_{(2)} \\ & - \dot{\hat{\mathbf{a}}}) - \frac{1}{\kappa_{\chi b}} \tilde{\chi}_b (\kappa_{\chi b} \frac{\partial \alpha_1}{\partial y} z_2 \omega_2 + \dot{\hat{\chi}}_b) \\ & + \frac{\partial \alpha_1}{\partial \hat{\mathbf{a}}} z_2 (\kappa_a (z_1 - \frac{\partial \alpha_1}{\partial y} z_2) \xi_{(2)} - \dot{\hat{\mathbf{a}}}) - (z_1 \\ & - \frac{\partial \alpha_1}{\partial y} z_2) d_{b2} - (\frac{3}{4l_1} + \frac{3}{4l_2}) \epsilon^T \epsilon + \frac{1}{\kappa_b} \tilde{b} (\kappa_b z_1 z_2 - \dot{\hat{b}}) \end{aligned} \tag{37}$$

The adaptive law for $\hat{b}$ is selected as

$$\dot{\hat{b}} = \kappa_b z_1 z_2. \tag{38}$$

Step j, $j = 3, 4, \cdots, n-1$***:*** Based on Step 2, Step j can be similarly obtained. The detail is omitted here due to the space limitation.

Step n: in this step, we have

$$\dot{z}_n = \dot{\hat{\chi}}_0 \omega_2^{(n-2)} + \hat{\chi}_0 \omega_2^{(n-1)} - \dot{\alpha}_{n-1}. \tag{39}$$

Note that

$$\hat{\chi}_0 \omega_2^{(n-1)} = \hat{\chi}_0 \frac{\delta^n + q_1 \delta^{n-1}}{\Lambda(\delta)} v_c(t) = \hat{\chi}_0 v_c(t) + v_0(t) \tag{40}$$

where

$$v_0(t) = - \frac{q_2 \delta^{n-2} + \cdots + q_n}{\Lambda(\delta)} v_c(t). \tag{41}$$

Eq. (39) can be rewritten as

$$\begin{aligned} \dot{z}_n = & \hat{\chi}_0 v_c(t) + KT_n - \frac{\partial \alpha_{n-1}}{\partial y} \mathbf{a}^T \xi_{(2)} - \frac{\partial \alpha_{n-1}}{\partial y} \chi_b \omega_2 \\ & + \frac{\partial \alpha_{n-1}}{\partial y} d_{b2} - \frac{\partial \alpha_{n-1}}{\partial y} \epsilon_2 - \frac{\partial \alpha_{n-1}}{\partial \hat{\mathbf{a}}} \dot{\hat{\mathbf{a}}} - \frac{\partial \alpha_{n-1}}{\partial \hat{\chi}_b} \dot{\hat{\chi}}_b \end{aligned} \tag{42}$$

where KT_n denotes the known terms in $\dot{z}_n$.

Therefore, the controller $v_c(t)$ is designed as

$$v_c(t) = \frac{1}{\hat{\chi}_0} v_s(t) \tag{43}$$

$$\begin{aligned} v_s(t) = & - KT_n - c_n z_n - z_{n-1} - l_n (\frac{\partial \alpha_{n-1}}{\partial y})^2 z_n \\ & + \frac{\partial \alpha_{n-1}}{\partial y} \hat{\mathbf{a}}^T \xi_{(2)} + \frac{\partial \alpha_{n-1}}{\partial y} \hat{\chi}_b \omega_2 \\ & + \frac{\partial \alpha_{n-1}}{\partial \hat{\mathbf{a}}} \kappa_a (z_1 - \Sigma_{i=1}^{n-1} \frac{\partial \alpha_i}{\partial y} z_{i+1}) \xi_{(2)} \\ & - \frac{\partial \alpha_{n-1}}{\partial \hat{\chi}_b} \kappa_{\chi b} (\Sigma_{i=1}^{n-1} \frac{\partial \alpha_i}{\partial y} z_{i+1}) \omega_2 \\ & - \kappa_a \frac{\partial \alpha_{n-1}}{\partial y} \xi_{(2)} (\Sigma_{i=1}^{n-2} \frac{\partial \alpha_i}{\partial \hat{\mathbf{a}}} z_{i+1}) \\ & - \kappa_{\chi b} \frac{\partial \alpha_{n-1}}{\partial y} \omega_2 (\Sigma_{i=2}^{n-2} \frac{\partial \alpha_i}{\partial \hat{\chi}_b} z_{i+1}) - z_{ss} \hat{D}_b \end{aligned}$$

where c_n and l_n are positive constants, $z_{ss} = |z_s|/z_n$ and $z_s = z_1 - \Sigma_{i=1}^{n-1} \frac{\partial \alpha_i}{\partial y} z_{i+1}$.

The adaptive laws for $\hat{\mathbf{a}}$, $\hat{\chi}_b$ and $\hat{D}_b$ are chosen as

$$\dot{\hat{\mathbf{a}}} = \kappa_a (z_1 - \Sigma_{i=1}^{n-1} \frac{\partial \alpha_i}{\partial y} z_{i+1}) \xi_{(2)}, \tag{44}$$

$$\dot{\hat{D}}_b = \kappa_{D_b} |z_s|, \tag{45}$$

$$\dot{\hat{\chi}}_b = -\kappa_{\chi b}(\Sigma_{i=1}^{n-1}\frac{\partial \alpha_i}{\partial y}z_{i+1})\omega_2 \tag{46}$$

where κ_a, $\kappa_{\chi b}$ and κ_{D_b} are positive constants.

Theorem 1. For the plant given in (1) with the hysteresis $\Pi(t)$ in (5), the inverse MGPI model $\hat{\Pi}^{-1}(t)$ in (10) and the inverse compensation error described as (15), the designed state observer (20), the adaptive output feedback controller specified by (43) and the adaptive laws (32), (33), (38), (44), (46), and (45) ensures that all the closed-loop signals are bounded and $y(t) \to y_d(t)$ as $t \to \infty$.

Proof. From (42)-(44), it can be obtained that

$$\begin{aligned}
\dot{z}_n =& -c_n z_n - z_{n-1} - l_n(\frac{\partial \alpha_{n-1}}{\partial y})^2 z_n - \frac{\partial \alpha_{n-1}}{\partial y}\tilde{\mathbf{a}}^T\xi_{(2)} \\
&- \frac{\partial \alpha_{n-1}}{\partial y}\tilde{\chi}_b\omega_2 + \frac{\partial \alpha_{n-1}}{\partial y}d_{b2} - \frac{\partial \alpha_{n-1}}{\partial y}\epsilon_2 \\
&+ \frac{\partial \alpha_{n-1}}{\partial \hat{\mathbf{a}}}(\kappa_a(z_1 - \Sigma_{i=1}^{n-1}\frac{\partial \alpha_i}{\partial y}z_{i+1})\xi_{(2)} - \dot{\hat{\mathbf{a}}}) \\
&- \frac{\partial \alpha_{n-1}}{\partial \hat{\chi}_b}(\kappa_{\chi b}(\Sigma_{i=1}^{n-1}\frac{\partial \alpha_i}{\partial y}z_{i+1})\omega_2 + \dot{\hat{\chi}}_b) \\
&- \kappa_a\frac{\partial \alpha_{n-1}}{\partial y}\xi_{(2)}(\Sigma_{i=1}^{n-2}\frac{\partial \alpha_i}{\partial \hat{\mathbf{a}}}z_{i+1}) \\
&- \kappa_{\chi b}\frac{\partial \alpha_{n-1}}{\partial y}\omega_2(\Sigma_{i=2}^{n-2}\frac{\partial \alpha_i}{\partial \hat{\chi}_b}z_{i+1}) - z_{ss}\hat{D}_b.
\end{aligned} \tag{47}$$

The Lyapunov function candidate V_n is selected as

$$V_n = V_{n-1} + \frac{1}{2}z_n^2 + \frac{1}{2\kappa_{D_b}}\tilde{D}_b^2 + \frac{1}{2l_n}\epsilon^T P_0 \epsilon. \tag{48}$$

The $\dot{V}_n$ is then obtained as

$$\begin{aligned}
\dot{V}_n \leq& -\Sigma_{i=1}^{n}c_i z_i^2 - (\Sigma_{i=1}^{n}\frac{3}{4l_i})\epsilon^T\epsilon \\
&+ \frac{1}{\kappa_a}\tilde{\mathbf{a}}(\kappa_a(z_1 - \Sigma_{i=1}^{n-1}\frac{\partial \alpha_i}{\partial y}z_{i+1})\xi_{(2)} - \dot{\hat{\mathbf{a}}}) \\
&- \frac{1}{\kappa_{\chi b}}\tilde{\chi}_b(\kappa_{\chi b}(\Sigma_{i=1}^{n-1}\frac{\partial \alpha_i}{\partial y}z_{i+1})\omega_2 + \dot{\hat{\chi}}_b) \\
&+ (\Sigma_{i=1}^{n-1}\frac{\partial \alpha_i}{\partial \hat{\mathbf{a}}}z_{i+1})(\kappa_a(z_1 - \Sigma_{i=1}^{n-1}\frac{\partial \alpha_i}{\partial y}z_{i+1})\xi_{(2)} - \dot{\hat{\mathbf{a}}}) \\
&- (\Sigma_{i=2}^{n-1}\frac{\partial \alpha_i}{\partial \hat{\chi}_b}z_{i+1})(\kappa_{\chi b}(\Sigma_{i=1}^{n-1}\frac{\partial \alpha_i}{\partial y}z_{i+1})\omega_2 + \dot{\hat{\chi}}_b) \\
&+ \frac{1}{\kappa_{D_b}}\tilde{D}_b(\dot{\tilde{D}}_b + \kappa_{D_b}|z_s|).
\end{aligned} \tag{49}$$

V_n is nonincreasing, it implies that z_i, for $i = 1, 2, \cdots, n$, $\hat{\mathbf{a}}$, $\hat{b}$, $\hat{\phi}$, $\hat{\chi}_0$, $\hat{\chi}_b$ and $\hat{D}_b$ are bounded. Furthermore, by applying the Lasalle-Yoshizawa theorem, it can be shown that $z_i \to 0$ $(i = 1, 2, \cdots, n)$ as $t \to \infty$, which implies that $y(t) \to y_d(t)$ as $t \to \infty$.

Based on the output feedback control developed in (43), the control signal $v(t)$, as shown in Fig. 1, for the plant given in (1) with the hysteresis $\Pi(t)$ in (5) is obtained by

$$v(t) = \hat{\Pi}^{-1}[v_c](t) \tag{50}$$

where $\hat{\Pi}^{-1}$ is given by (10).

6. SIMULATION RESULTS

In this section, the effectiveness of the proposed controller is verified by two simulation examples.

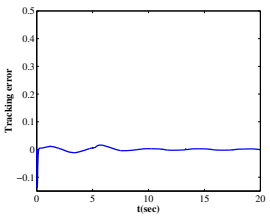

Fig. 2. The tracking error.

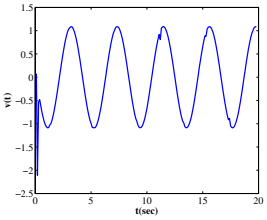

Fig. 3. The controller signal.

6.1 Example 1:

In the first example, a linear system with unknown parameters is considered, which can be described by

$$\ddot{x} = ax + bu(t), \qquad y = x \tag{51}$$

where $u(t)$ stands for the output of the compensated hysteresis output (18). The parameter a and b are selected as $a = 1$ and $b = 1$ and assumed to be unknown in the simulation. The desired trajectory is given as $y_d(t) = 5sin(1.5t)$. The initial state of the system is $x(0) = 0$ and the sample time is 0.0001. p_{m0} and $\hat{p}_{m0}$ are chosen as 0.5 and 0.52. The thresholds of the MGPI model is selected as $r_i = 0.3 * i$, for $i = 1, 2, \cdots, 10$. The actual and estimated density function of the MGPI model $\Pi(t)$ and $\hat{\Pi}(t)$ are $p_m(r) = 0.5e^{-0.0014r^2}$ and $\hat{p}_m(r) = 0.52e^{-0.002r^2}$, respectively, and the envelope function parameter is chosen as $m_0 = 1.7$. For the state observer, the parameter q is selected as $q = [q_1, q_2]^T = [1, 3]^T$. The control parameters are summarized in Table 1.

Table 1. Controller Parameters in Example 1

c_1	125.598	c_2	189.475	1_1	0.0003	l_2	0.0003
$\hat{a}(0)$	0.6	κ_a	0.0008	$\hat{b}(0)$	0.75	κ_b	0.028
$\hat{\chi}_0(0)$	1.4	$\kappa_{\chi 0}$	0.0005	$\hat{\chi}_b(0)$	0.3	$\kappa_{\chi b}$	0.001
$\hat{\phi}(0)$	1.3	κ_ϕ	0.457	$\hat{D}_b(0)$	0.01	κ_{D_b}	0.0001

Fig. 2 and 3 show the tracking error and the control signal, respectively. The comparison between the desired trajectory $y_d(t)$ and the actual system output $y(t)$ can be found in Fig. 4. The simulation results demonstrate that the developed control algorithm can effectively compensate the effect of hysteresis as well as achieve admirable tracking accuracy.

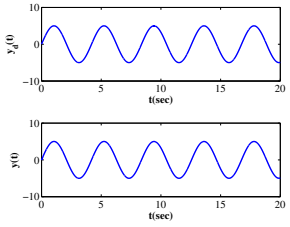

Fig. 4. The desired output $y_d(t)$ and the actual output $y(t)$.

6.2 Example 2:

An second order nonlinear plant preceded by a hysteresis actuator is considered in the second example. The nonlinear system is described as

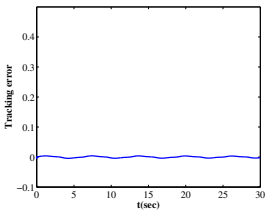

Fig. 5. The tracking error.

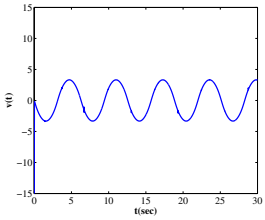

Fig. 6. The controller signal.

$$\ddot{x} = a\frac{1-e^{-x(t)}}{1+e^{-x(t)}} + bu(t), \qquad y = x \tag{52}$$

where $u(t)$ stands for the output of the compensated hysteresis output (18). The parameter a and b are selected as $a = 1$ and $b = 1$ and assumed to be unknown in the simulation. The desired trajectory is given as $y_d(t) = 4sin(t)$. The initial state of the system, sampling time, the parameters of MGPI model, and the observer parameters are the same as in example 1. The control parameters are summarized in Table 2.

Table 2. Controller Parameters in Example 2

c_1	120.961	c_2	99.2	1_1	0.0003	l_2	0.0003
$\hat{a}(0)$	0.02	κ_a	0.0045	$\hat{b}(0)$	0.75	κ_b	0.032
$\hat{\chi}_0(0)$	1.4	$\kappa_{\chi 0}$	0.005	$\hat{\chi}_b(0)$	0.3	$\kappa_{\chi b}$	0.0125
$\hat{\phi}(0)$	1.3	κ_ϕ	0.452	$\hat{D}_b(0)$	0.01	κ_{D_b}	0.004

The simulation results presented in Fig. 5, 6 and 7 are the tracking error, the control signal $v(t)$ and the comparison of the desired output $y_d(t)$ and the actual system output $y(t)$, respectively. It can be seen that the proposed output feedback controller by considering the inverse compensation error demonstrates excellent tracking performance.

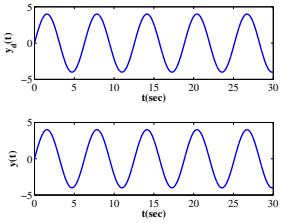

Fig. 7. The desired output $y_d(t)$ and the actual output $y(t)$.

7. CONCLUSION

In this paper, an output feedback control scheme has been proposed with the inverse compensation for a class of uncertain systems preceded by smart material base actuators with hysteresis effects. For doing so, an analytical expression of the inverse compensation error has been derived and an observer has been designed for the state estimation. The proposed control method not only guarantee the stability of the close-loop control system, but also ensure the desired tracking accuracy. The effectiveness of the developed controller is illustrated by the simulation studies.

REFERENCES

G. Tao and P. V. Kokotovic Adaptive control of plants with unknown hysteresis. *IEEE Transaction on Automatic Control*, volume 40, number 2, pages 200-212, 1995.

I. D. Mayergoyz, *Mathematical models of hysteresis*. Spring-Verlag, New York, 1991.

M. Krasnoselskii and A. Pokrovskii *Systems with hysteresis*. Springer, Moscow, 1989.

X. Tan and J. S. Baras Modeling and control of hysteresis in magnetostrictive actuators. *Automatica*, volume 40, number 9, pages 1469-1480, 2004.

S. Liu and C. Y. Su A modified generalized Prandtl-Ishlinskii model and its inverse for hysteresis compensation. *American Control Conference (ACC)*, Washington DC, USA, pages 4759-4764, 2013.

X. Chen, T. Hisayama and C. Y. Su Adaptive control for uncertain continuous-time systems using implicit inversion of prandtl-ishlinskii hysteresis representation. *IEEE Transactions on Automatic Control*, volume 55, number 10, pages 2357-2363, 2010.

P. Krejci and K. Kuhnen Inverse control of systems with hysteresis and creep. *IEE Proceedings of Control Theory and Applications*, volume 148, number 3, pages 185-192, 2001.

C. Y. Su, Q. Wang, X. Chen and S. Rakheja Adaptive variable structure control of a class of nonlinear systems with unknown Prandtl-Ishlinskii hysteresis *IEEE Transactions on Automatic Control*, volume 50, number 12, pages 2069-2074, 2005.

P. Krejci *Hysteresis, Convexity and Dissipation in Hyperbolic Equations*. Gakkotosho, Tokyo, 1996.

S. Liu and C.-Y. Su A note on the properties of a generalized Prandtl-Ishlinskii model. *Journal of Smart Materials and Structures*, volume 20, number 8, pages 1-6, 2011.

M. Al Janaideh, S. Rakheja and C.-Y. Su A generalized Prandtl-Ishlinskii model for characterizing the hysteresis and saturation nonlinearities of smart actuators. *Journal of Smart Materials and Structures*, volume 18, number 4, pages 1-9, 2009.

M. Brokate and J. Sprekels *Hysteresis and Phase Transitions*. Spring-Verlag, New York, 1996.

Q. Wang and C.-Y. Su Robust adaptive control of a class of nonlinear systems including actuator hysteresis with Prandtl-Ishlinskii presentations. *Automatica*, volume 42, number 5, pages 859-867, 2006.

S. Liu, X. Sheng, Z. Li and C. Y. Su Inverse control of a class of nonlinear systems with modified generalized Prandtl-Ishlinskii hysteresis. *in the proceedings of the 38th Annual Conference on IEEE Industrial Electronics Society (IECON)*, Montreal, QC, Canada, pages 2319-2324, 2012.

J. Zhou, C. Wen and Y. Zhang Adaptive backstepping control of a class of uncertain nonlinear systems with unknown backlash-like hysteresis. *IEEE Transaction on Automatic Control*, volume 49, number 10, pages 1751-1757, 2004.

J. Zhou, C. Wen and T. Li Adaptive output feedback control of uncertain nonlinear systems with hysteresis nonlinearity. *IEEE Transaction on Automatic Control*, volume 57, number 10, pages 2627-2633, 2012.